Jour. Fac. Sci., Hokkaido Univ., Ser. VII (Geophysics), Vol. 11, No. 1, 51-70, 1998.

A Case Study and Numerical Simulation of Polar Low in the Labrador Sea

Kazuhisa Tsuboki

Institute for Hydrospheric-Atmospheric Sciences, Nagoya University, Nagoya, 464-8601, Japan

(Received November 30, 1997)

Abstract

A polar low over the Labrador Sea was observed on 14-15 February 1992. Satellite images obtained from AVHRR showed a cyclogenesis and development of the polar low. The cloud streaks over the Labrador Sea suggested that a convergence formed between the westerly from Eastern Canada and the northeasterly from Greenland when the polar low generated. A vortex formed along the convergence zone and developed into the polar low of which horizontal diameter was about 500 km.

On the basis of the JMA global objective analysis (GANAL), an intense upper cold vortex was located over the Labrador Sea when the polar low developed. The GANAL data showed a dry and cold westerly was prevailing over the Labrador Sea and that the convergence occurred between the westerly from Eastern Canada and the northeasterly from Greenland. The polar low formed along the convergence zone. The polar low was shallow disturbance which was confined to below 700 hPa.

In order to clarify the detailed structure and the processes of cyclogenesis and development of the polar low, we made a numerical simulation experiment using the Japan Spectral Model. The simulation showed that a convergence occurred between the westerly from Eastern Canada and the northeasterly from Greenland and that the polar low developed along the convergence zone. There was a strong stable layer above 700 hPa and the disturbance of the polar low was confined to below 700 hPa.

As far as this case of the Labrador polar low, we could infer that the convergence was important for the cyclogenesis and that latent and sensible heat fluxes were important for the development of the polar low.

1. Introduction

A polar low is a mesoscale cyclone generated and developed in a cold air streams of the polar airmass north of the major Polar Front. Its horizontal scale is 100~1000 km and it usually forms over the sea. Since polar lows develop rapidly over sea and have their small horizontal size, the prediction of polar low genesis is difficult (Rasmussen and Lystad, 1987). Polar lows bring a severe weather to a coastal region and its prediction is, therefore, important.

Polar lows have been observed in middle and high latitude seas and have been intensively investigated. In particular, they were observed in the North Atlantic Ocean, the North Pacific Ocean (Sardie and Warner, 1985 ; Reed, 1989 ; Reed and Blier, 1986a, 1986b), the Norwegian Sea, the North Sea, the Barents Sea (Rasmussen, 1985 ; Businger, 1985), the Gulf of Alaska, and the Bering Sea (Businger, 1987 ; Businger and Walter, 1988). Polar lows are also observed in the Sea of Japan (Asai and Miura, 1981 ; Ninomiya, 1989 ; Tsuboki and Wakahama, 1992).

Two types of instability of the atmosphere are considered to be important for the development mechanism of polar lows ; one is baroclinic instability (Harrold and Browning, 1969 ; Mansfield, 1974 ; Duncan, 1977 ; Reed and Duncan, 1987) and the other is conditional instability of the second kind (CISK) (Rasmussen, 1979 ; Bratseth, 1985 ; Økland, 1987 ; Craig and Cho, 1988). Mansfield (1974), using the Eady (1949) model with baroclinicity confined to below a lid at 1.6 km, showed that if baroclinic waves are shallow, then the wavelength of the most unstable wave is ~600 km ; this is similar to the observed wavelength of polar lows. Duncan (1977) used a quasi-geostrophic numerical model with low static stability near the earth's surface and found unstable modes which have similar dimensions to polar lows. He concluded that conversion of available potential energy to eddy kinetic energy occurs in the lowest 200 or 300 hPa of the atmosphere when the low-level static stability is small. Reed (1979) concluded that polar lows are primarily a baroclinic phenomenon while CISK and barotropic instability cannot be ruled out as possible forcings. Sardie and Warner (1983) developed a three-layer, two-dimensional, quasi-geostrophic model which includes both the effects of latent heating and baroclinicity, and found that moist baroclinic processes alone may explain the origin of Pacific polar lows, while moist baroclinicity and CISK are essential for the genesis of Atlantic polar lows. Sardie and Warner (1985) also used a numerical model to find that moist baroclinicity and CISK are both important in the genesis of the Atlantic and Pacific polar lows. Orlanski (1986) used a two-dimensional model to solve the initial value problem describing the evolution of disturbances on a mean baroclinic state and demonstrated the importance of localized surface heating in producing the more intense development of short baroclinic waves. He also showed that the shallow mesoscale baroclinic wave will explosively develop into a deep intense system with the addition of moisture. Nakamura (1988) investigated the effects of stratification and nongeostrophy and found that both mesoscale waves trapped in the lower

layer with a small static stability and long waves extending throughout the atmosphere are unstable. Ninomiya (1989) studied the polar low and comma cloud over the Japan Sea (45-35°N) and the northwestern Pacific Ocean (55-40° N) in winter and found that they develop in a zone 500-1000 km north of the major polar frontal zone, where baroclinicity in the lower-middle troposphere is strong. Tsuboki and Wakahama (1992) proposed a baroclinic instability as a mechanism of the Hokkaido polar low.

The Labrador Sea is a region where polar lows frequently develop in winter. They were also investigated observationally (Forsythe and Haar, 1996) and numerically (Mailhot et al., 1996). In order to study storms including polar lows along the east coast of Canada, the Canadian Atlantic Storms Program II (CASP II) were conducted from January to March 1992. During this program, several cases of the Labrador polar low were observed.

A significant case of a polar low was observed off the west coast of Greenland on 14-15 February 1992. Moore et al. (1996) described results of a case study of this polar low. In this paper, we will present characteristics of the Labrador polar low obtained from data analysis and a numerical simulation experiment.

2. Data and numerical model

The following data for the period from 10 to 17 February 1992 were provided by the Japan Meteorological Agency (JMA) and were used for data analyses and numerical modelings;

1. the global objective analysis (GANAL) with a resolution of 1.875 degrees in both latitude and longitude, and 15 levels every 6 hours,
2. climatological data of the global sea surface temperature (SST) with a resolution of 1.0 degrees in both latitude and longitude,
3. and sea surface temperature of the Labrador Sea and the North Atlantic Ocean.

The global objective analysis data were interpolated into model grids and used for initial and boundary conditions of numerical simulations. The climatological SST data gave a lower boundary condition in sea areas.

The satellite images of the Advanced Very High Resolution Radiometer (AVHRR) were received by Department of Physics, University of Toronto and were provided to use in this study.

We adapted the Japan Spectral Model (JSM) of version of 1988 for a simulation of the Labrador polar low. JSM which was developed by JMA for

operational forecasts is a spectral limited-area model (Segami et al., 1989). The model is formulated in terms of the primitive equations in sigma coordinates. The spectral method with a time-dependent lateral boundary condition (Tatsumi, 1986) is adopted in the model. The vertical levels were 23 sigma levels in this study. The model expresses horizontal fields of model variables by the double Fourier series. The transform grids were 129 and 129 points in the zonal and meridional directions, respectively. The horizontal spacing of model grids was chosen to be 60 km for the present study. The domain of the model covered the northern Atlantic and the North America (Fig. 1). The map projection was the North Polar Stereographic Projection. The distribution of the sea surface temperature which was fixed throughout the integration period was climatological value.

Moist processes in the model were the moist convective adjustment for subgrid-scale convection, large-scale condensation and evaporation of rain-

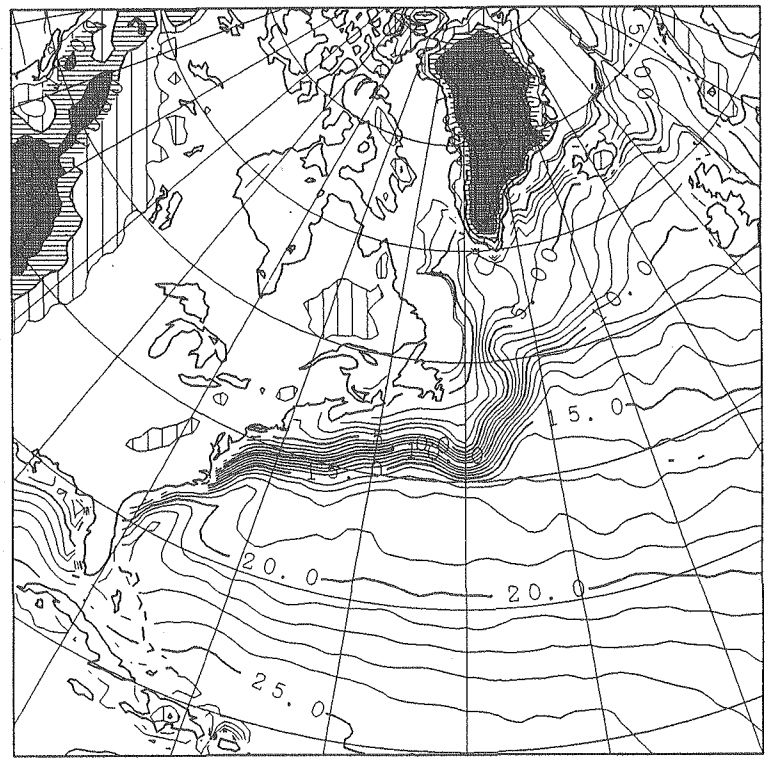

Fig. 1. The topography and the sea surface temperature (°C) on 14 February 1992 in the simulation domain.

drops. Surface fluxes were calculated by a bulk method. The level two version of the turbulent closure model (Mellor and Yamada, 1974) was used for vertical diffusions. Temperature of ground was calculated by a four-layer model. Radiation was taken into account only for the calculation of ground temperature.

3. A case study of the Labrador polar low

The Labrador Sea is located in the northern part of the Atlantic Ocean between Eastern Canada and Greenland. The sea is located around 50°N to 60° N and 50°W to 60°W. While the coastal region of East Canada is covered with sea ice, most of the Labrador Sea is open even in the middle of winter. Greenland is a plateau as high as 3 km in altitude. It, therefore, strongly influences the weather in that area.

During winter time, an intense cold air outbreak occasionally occurs along the coast of Eastern Canada. The wind from the continent is cold and dry. Its temperature sometimes attains about −30°C while the sea surface temperature ranges from 0°C to 5°C in the Labrador Sea. This large temperature difference and intense wind speed cause large latent and sensible heat fluxes from the sea. As a result, a mixing layer rapidly develops in the lower troposphere when the cold air outbreak occurs over the sea.

A polar low in the Labrador Sea develops in such synoptic environment. A significant case of the Labrador polar low observed on 14-15 February 1992. Time series of satellite images (not shown) observed by NOAA AVHRR shows cloud patterns associated with development of the polar low. A number of thin cloud streaks associated with the cold air outbreak extended over the Labrador Sea from the edge of the sea ice at 0714 UTC, 14 February 1992. An intensively active cloud region indicated by low IR (infrared) Tbb (the equivalent black body temperature) is present between Labrador and Greenland. Convective activity in the active cloud region became intense at 1142 UTC, 14 February. The cloud area was elongated to the east and a vortex pattern of cloud became significant at 1706 UTC, 14 February. The vortex cloud developed and moved eastward during the period from 2211 UTC, 14 February 1992 to 1122 UTC, 15 February. It was in a mature stage at 1650 UTC, 15 February (Fig. 2) with a clear eye to the west of Greenland and a long trail which extended to the west from the vortex cloud. The diameter of the vortex was about 500 km. A synoptic low moved to the southeast of Greenland. The polar low began to decay at 1830 UTC, 15 February and the vortex cloud destroyed at 2245 UTC,

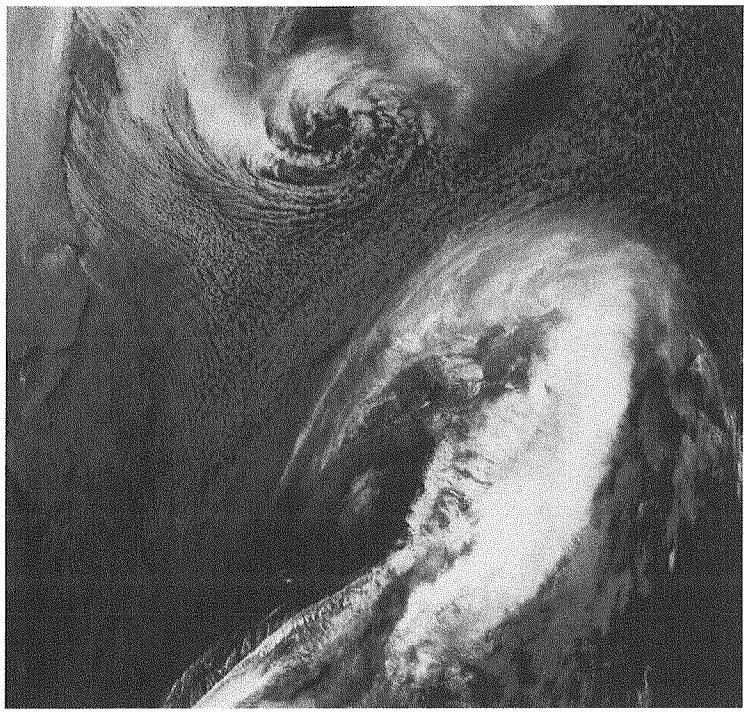

Fig. 2. Infrared image observed by NOAA AVHRR at 1650 UTC, 15 February 1992. A vortex cloud of the mature polar low is located to the west of Greenland and a large cloud area of the synoptic low is extending over the North Atlantic Ocean.

15 February. Finally, the polar low dissipated 0651 UTC, 16 February 1992.

A close view (not shown) of the developing polar low showed an active cloud region. We will refer to the active cloud band as "the band cloud". The cloud streaks on the south side of the band cloud were elongated from the west to the east. On the other hand, the cloud streaks on the north side of the band cloud extended from the northwest to the south in the west half area and from the northeast to southwest in the east half area. These cloud patterns suggest that the cloud band caused by a convergence between the three air streams.

The JMA global objective analysis (GANAL) shows the synoptic pattern when the polar low occurred. Figure 3 shows the surface pressure and the surface wind field from 1800 UTC, 14 February 1992 to 1800 UTC, 15 February 1992 every 12 hours. A stationary synoptic low was located along the east coast of Greenland. Another synoptic low moved northeastward passing over Newfoundland and finally merged with the stationary low. A cold northwester-

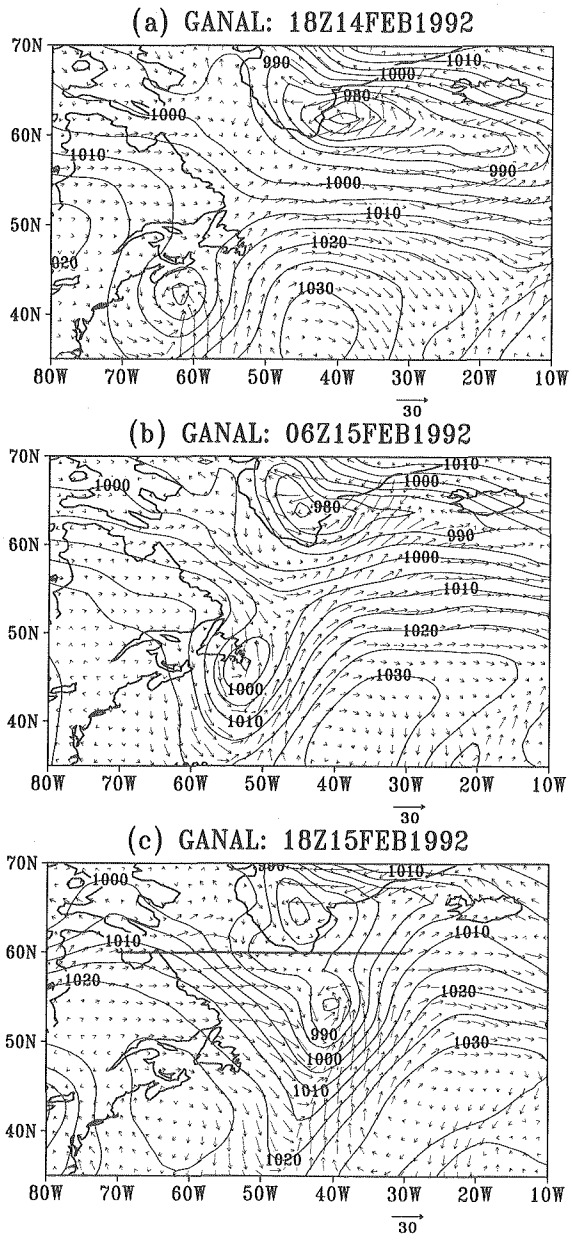

Fig. 3. Surface pressure (contours in hPa) and surface wind vectors at (a) 1800 UTC, 14 February 1992, (b) 0600 UTC, 15 February 1992 and (c) 1800 UTC, 15 February 1992 obtained from the JMA global objective analysis. The line in (c) along 60°N indicates the position of the vertical cross sections in Fig. 4.

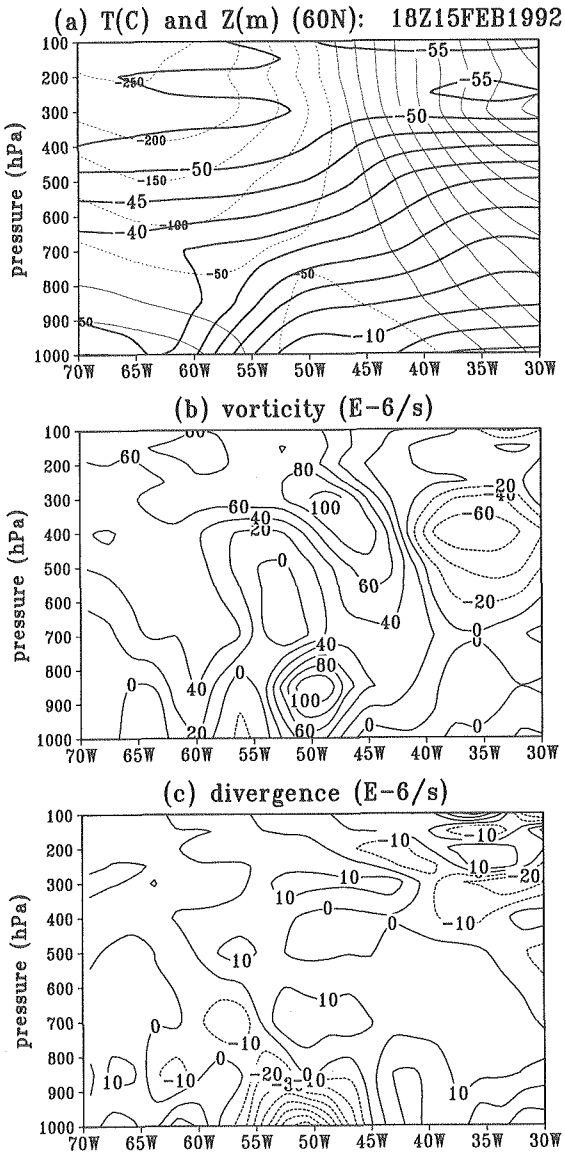

Fig. 4. Vertical cross sections along 60°N at 1800 UTC, 15 February 1992 of (a) height deviation from the averaged height between 30°W and 70°W (thin lines in meter) and temperature (thick lines in °C), (b) vorticity (10^{-6} s^{-1}), and (c) divergence (10^{-6} s^{-1}).

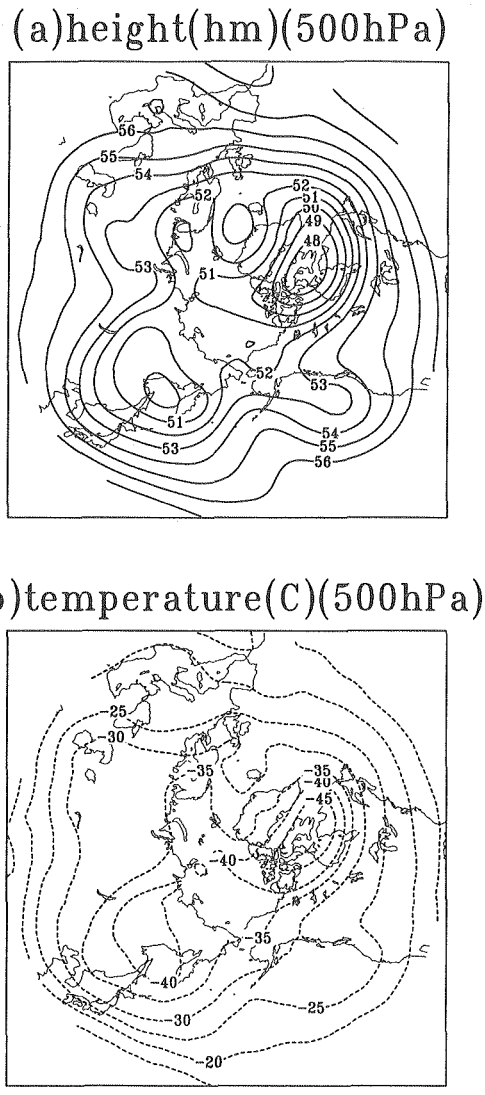

Fig. 5. (a) Averaged height field (hm) and (b) averaged temperature field (°C) of 500 hPa during the period from 0000 UTC, 13 February 1992 to 0000 UTC, 16 February 1992.

ly became intense to the west of these synoptic lows. A convergence between the westerly from Eastern Canada and the northerly from Greenland is significant over the Labrador Sea at 0600 UTC, 15 February 1992 (Fig. 3b). A weak mesoscale low formed to the southwest of the Greenland at 1800 UTC, 15

February 1992 (Fig. 3c). This corresponds to the polar low under consideration.

The vertical cross sections of height deviation and temperature along 60°N (Fig. 4a) show a shallow low which confined to below 700 hPa between 50°W and 40°W. The horizontal gradient of temperature was intense below 700 hPa between 60°W and 50°W which was formed owing to airmass transformation when the cold air moved from the continent to the sea. A significant positive vorticity (Fig. 4b) and a negative divergence (Fig. 4c) were present below 700 hPa between 55°W and 45°W. These correspond to the polar low observed by the satellite.

Figure 4a also shows that the polar low was located below the upper cold low. The averaged height field at 500 hPa during the period from 0000 UTC, 13 February 1992 to 0000 UTC, 16 February 1992 (Fig. 5) shows a significant cold low was located over the Labrador Sea. This is a significant characteristic feature of the environment of the polar low development. Another upper cold low at 500 hPa was located over the northern Japan. A polar low occasionally occurs in the northern part of the Sea of Japan in such environment.

On the basis of the data analysis, we could infer that the polar low was a shallow mesoscale low which developed below the large-scale upper cold low.

4. Numerical simulation of the Labrador polar low

In order to examine a detailed structure of the polar low observed 14-15 February 1992 in the Labrador Sea, we performed a prediction experiment. The initial value of the simulation was given by GANAL at 0000 UTC, 15 February 1992.

The prediction experiment simulated well the observed behavior of the synoptic lows. The patterns of the surface pressure and surface flow (Fig. 6) show that the stationary synoptic low was located at the southernmost part of Greenland and the other synoptic low moved northeastward passing over Newfoundland. These lows merged into a single low at 2000 UTC, 15 February 1992. The surface flow pattern shows that a convergence formed to the southwest of Greenland at 0400 UTC, 15 February 1992. A weak mesoscale low also began to develop to the southwest of the southernmost part of Greenland. The convergence and the mesoscale low developed with time and the low was in mature stage at 1600 UTC, 15 February 1992. This mesoscale low is considered to correspond to the observed polar low.

The vorticity field at 925 hPa also shows development of the polar low. The vorticity to the southwest of Greenland intensified during the period from

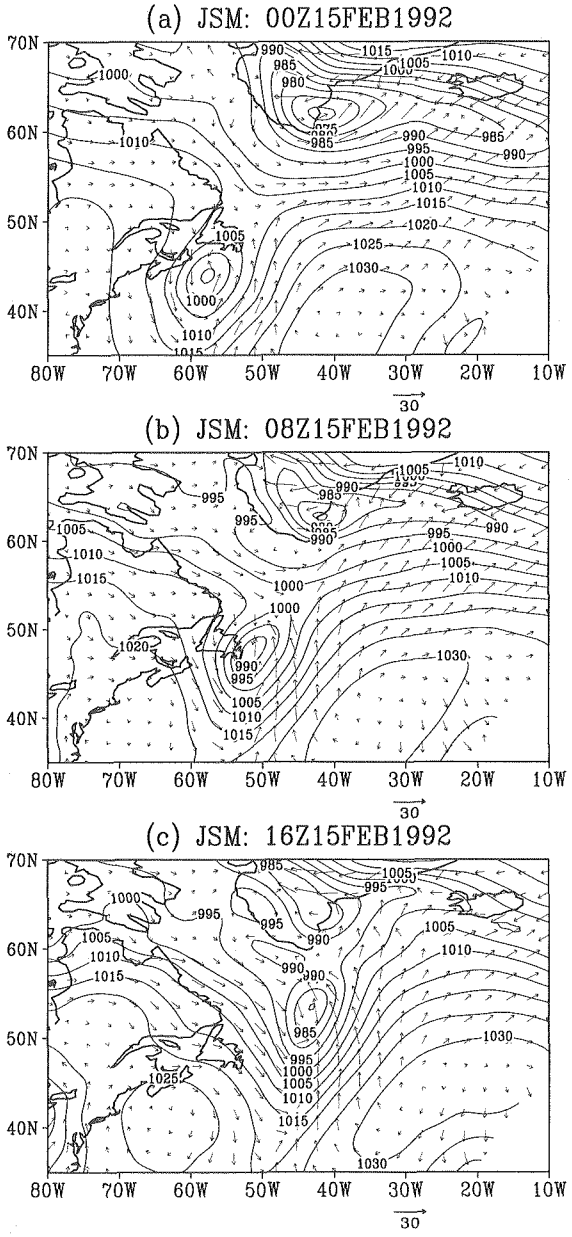

Fig. 6. Surface pressure (contours in hPa) and surface wind vectors at (a) 0000 UTC, 15 February 1992, (b) 0800 UTC, 15 February 1992 and (c) 1600 UTC, 15 February 1992 obtained from the JSM prediction experiment.

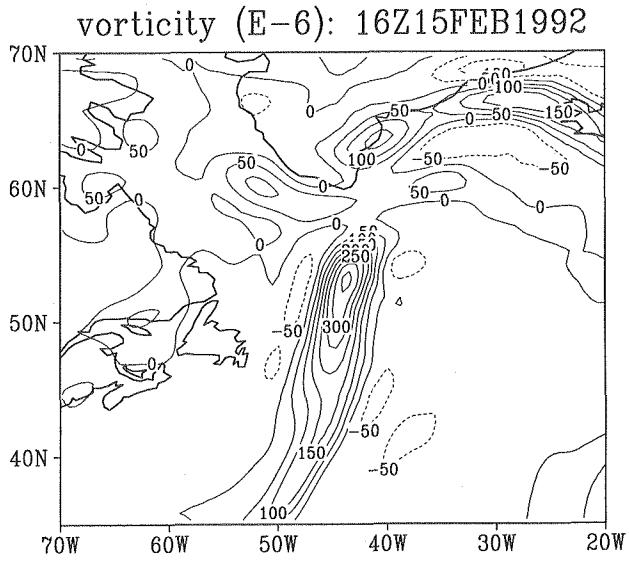

Fig. 7. Vorticity (10^{-6} s^{-1}) of 925 hPa predicted by JSM at 1600 UTC, 15 February 1992.

0400 to 1200 UTC, 15 February 1992 and attained its maximum at 1600 UTC, 15 February 1992 (Fig. 7).

Figure 8 shows time-height cross sections of vorticity and divergence averaged in the area of 57°W, 47°W, 58°N, and 63°N, where the polar low developed. The averaged vorticity (Fig. 8a) below 700 hPa increased with time. It maximum was present at a level of 925 hPa. On the other hand, the averaged vorticity above 700 hPa was almost constant with time. The time-height cross section of divergence (Fig. 8b) shows a significant negative divergence below 800 hPa and positive divergence around 700 hPa. The low level negative divergence was most intense during the period from 0900 to 1500 UTC, 15 February 1992. The polar low was in mature stage during this period.

The time-height cross section of potential temperature (Fig. 9) shows that a mixing layer developed below 700 hPa and a strong stable layer was present above 700 hPa during the period of the development of the polar low. This indicated that essential part of the polar low was confined to below 700 hPa. The polar low was, therefore, a shallow disturbance.

The vertical cross sections of vorticity, potential temperature and specific humidity along 60°N at 1600 UTC, 15 February 1992 obtained from the result of the prediction experiment are shown in Fig. 10. The maximum of vorticity was present between 47°W and 55°W below 800 hPa which corresponds to the polar

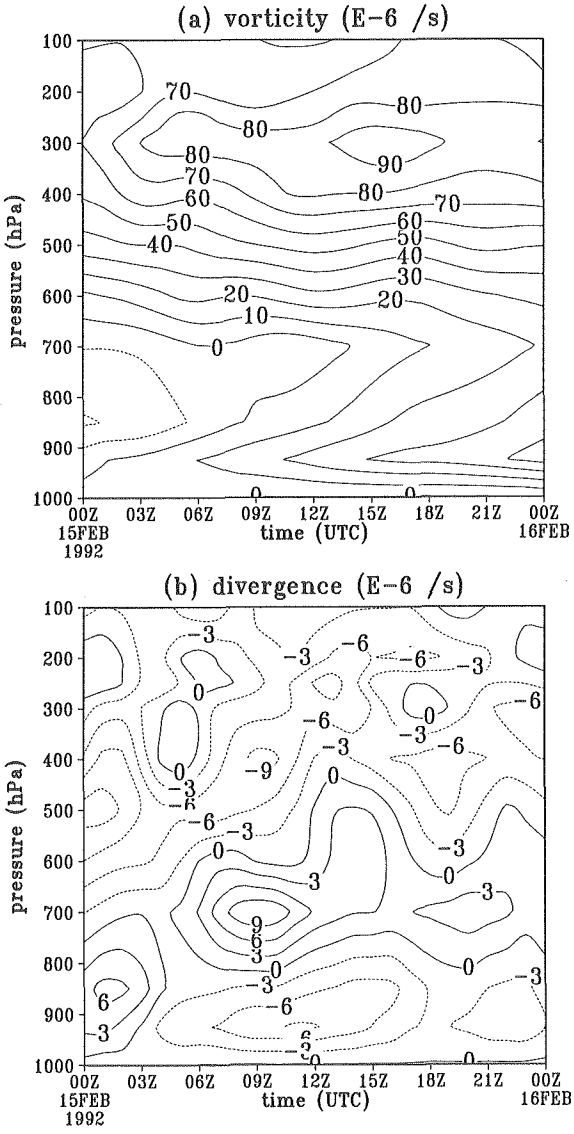

Fig. 8. Time-height cross sections of (a) vorticity (10^{-6} s^{-1}) and (b) divergence ($10^{-6}s^{-1}$) averaged in the area of 57°W, 47°W, 58°N and 63°N obtained from the JSM prediction experiment.

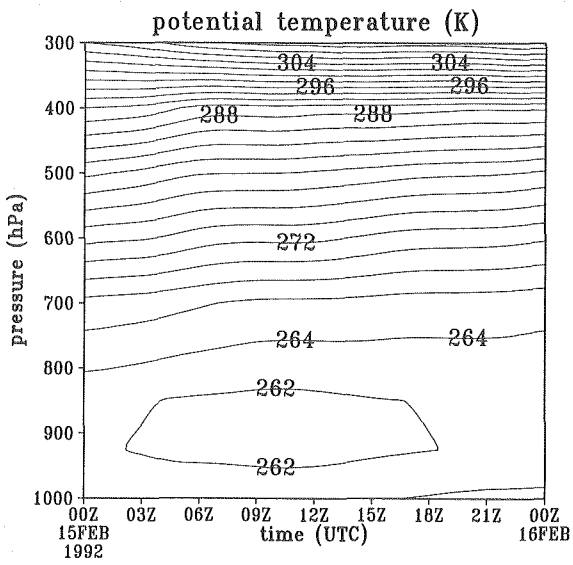

Fig. 9. Time-height cross section of potential temperature (K) averaged in the area of 57°W, 47°W, 58°N and 63°N obtained from the JSM prediction experiment.

low. Its maximum was located at 925 hPa and most part of the disturbance was confined to below 750 hPa. There was significant positive vorticity above the polar low, which corresponds to the upper cold low. The vertical cross section of potential temperature shows that the polar low developed in the shallow mixing layer where the horizontal temperature gradient was large in the lower troposphere. The vertical cross sections of the potential temperature and specific humidity show that an intense transformation of cold airmass occurred below 700 hPa when the cold and dry continental airmass moved to over the Labrador Sea. The coast of East Canada was located around 65°W. The stability of the atmosphere rapidly decreased below 700 hPa and the moisture increased with distance from the coast.

This rapid airmass transformation was caused by large latent and sensible heat fluxes from the sea. Figure 11 shows distributions of the latent and sensible heat fluxes at the surface. The latent heat flux was large in the Labrador Sea. Its maximum value was about 150 Wm^{-2}. The sensible heat flux was about 150~250 Wm^{-2} at the central part of the Labrador Sea. These large heat fluxes supplied heat and moisture to the atmosphere and intense airmass transformation occurred over the Labrador Sea. Consequently, the mixing layer developed rapidly in the lower troposphere.

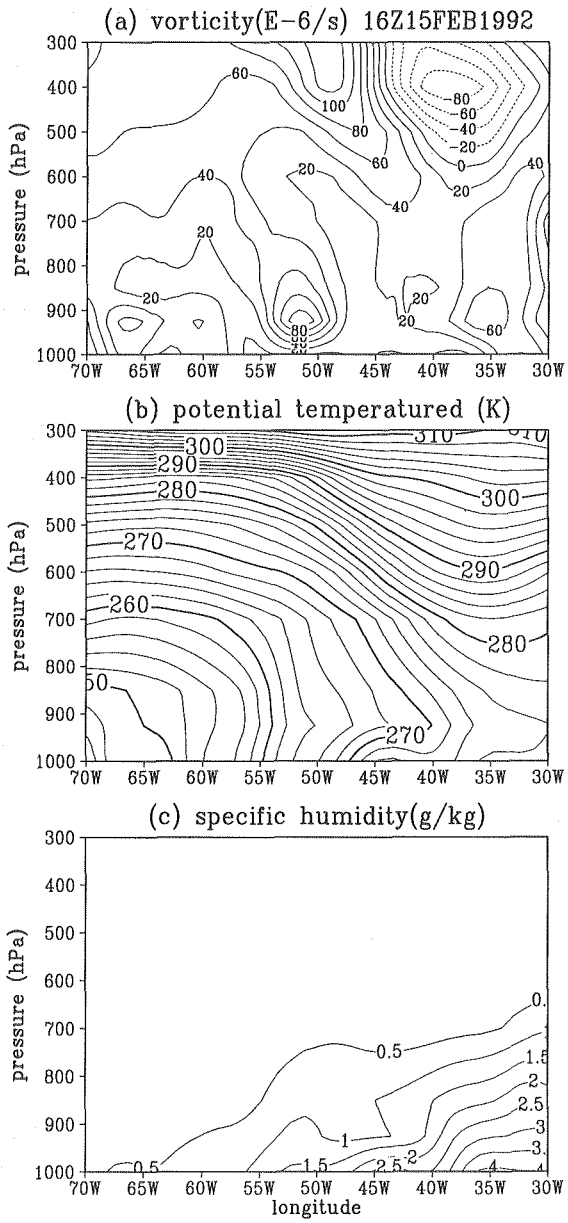

Fig. 10. Vertical cross sections along 60°N at 1600 UTC, 15 February 1992 of (a) vorticity (10^{-6} s^{-1}), (b) potential temperature (K) and (c) specific humidity (g kg^{-1}) obtained from the JSM prediction experiment.

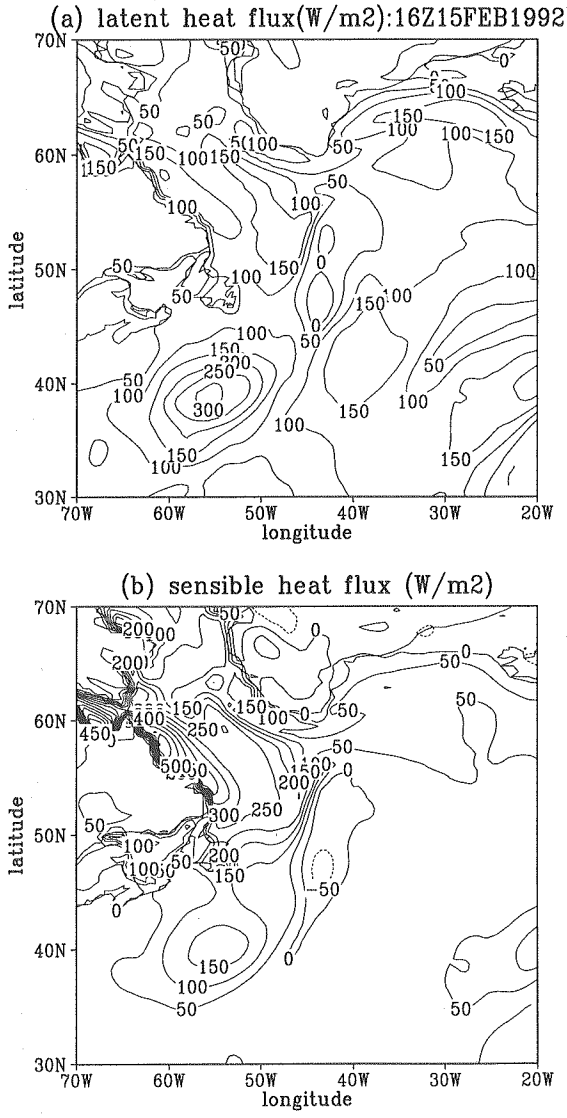

Fig. 11. (a) Latent heat flux (Wm^{-2}) and (b) sensible heat flux (Wm^{-2}) at surface predicted by JSM at 1600 UTC, 15 February 1992.

5. Discussion

5.1 Validation of the simulation experiments

The prediction experiment using JSM simulated properly the polar low

observed on 15 February 1992 in the Labrador Sea. The simulated low had a similar horizontal scale to the observed polar low and was located in the same position of the polar low. The vertical extension was shallow because the intense stable layer was present above 700 hPa and the disturbance in the lower troposphere was not able to extend into the stable layer.

The satellite images show that convergence occurred between the westerly from Eastern Canada and the northeasterly from Greenland at the beginning of the development of the polar low. The simulation also showed the similar convergence when the polar low began to develop.

The satellite images shows the convergence and vigorous cloud had already begun to develop on 14 February 1992. On the contrary, prediction experiments which started at 0000 UTC and 1800 UTC, 14 February 1992 did not simulate this convergence and the polar low. These suggest that the simulation of the polar low was sensitive to the initial data and initial disturbance could be necessary for the simulation of this polar low.

5.2 Similarities between the Labrador polar low and Hokkaido polar low

The northernmost part of the Sea of Japan is a region where a polar low is frequently observed during winter time. Since the polar low usually forms off the west coast of Hokkaido, we will refer to the polar low as "the Hokkaido polar low". There are many common features between the Labrador polar low and the Hokkaido polar low;

- their horizontal scales of both polar lows are several hundred kilometers,
- they are a shallow disturbance which confined to the lower troposphere,
- they occur over the sea adjacent to a land where horizontal temperature gradient is large,
- latent and sensible heat fluxes from the sea are important for their development,
- they develop along a convergence zone at their beginning of development,
- they occur in the region where the horizontal temperature gradient is strong in the lower troposphere,
- and they often accompany an upper cold vortices.

In the case of present study, upper cold vortices were located over the Labrador Sea and the northern part of the Sea of Japan (Fig. 5). We could consider that the Labrador polar low and the Hokkaido polar low are similar type of mesoscale cyclones.

5.3 Possible mechanism

As far as this case of the Labrador polar low, we could infer that the convergence was important for the cyclogenesis and that the latent and sensible heat fluxes were important for the development. It is not clear presently the role of the upper cold vortex in the cyclogenesis of the polar low. In order to clarify the mechanism of cyclogenesis and development of the Labrador polar low, we need further numerical experiment and detailed examination of the results.

6. Summary and conclusions

When a cold air outbreak occurs over the Labrador Sea, a polar low occasionally forms in the cold polar air stream over the Labrador Sea. An significant case of the Labrador polar low was observed on 14-15 February 1992. We made a case study of the polar low.

Satellite images obtained from NOAA AVHRR showed the cyclogenesis and development of the polar low. According to cloud streaks over the Labrador Sea, a convergence between the westerly from Eastern Canada and the northeasterly from Greenland occurred when the polar low began to develop. A vortex formed along the convergence zone and developed into the polar low of which the horizontal diameter was about 500 km.

On the basis of the JMA global objective analysis, we found the synoptic condition for the development of the polar low. An intense upper cold vortex was located over the Labrador Sea when the polar low occurred. A dry and cold westerly was prevailing over the Labrador Sea. A convergence occurred between the westerly from Eastern Canada and the northeasterly from Greenland. The polar low formed along the convergence zone. The polar low was a shallow disturbance which was confined to below 700 hPa.

In order to clarify the detailed structure and the processes of cyclogenesis and development, we made numerical prediction experiments using the Japan Spectral Model. JSM simulated well the development of the Labrador polar low. A convergence occurs between the westerly from Eastern Canada and the northeasterly from Greenland. Then, the polar low developed along the convergence zone. There was a strong stable layer above 700 hPa and the simulated polar low was also confined to below 700 hPa.

A similar type of the polar low is occasionally occurs in the northern part of the Sea of Japan. We pointed out common features between the Labrador

and Hokkaido polar lows.

As far as this case of the Labrador polar low, we could infer that the convergence was important for the cyclogenesis and that the latent and sensible heat fluxes were important for the development. It is not clear presently the role of the upper cold vortex in the cyclogenesis of the polar low.

Acknowledgments

The author would like to express his sincere thanks to Professor T. Asai, Professor R. Kimura and Dr. K. Nakamura of the Ocean Research Institute (ORI), University of Tokyo for their encouragement and indispensable assistance throughout this work. The author would like to thank Professor W. Richard Pelteir and Professor G.W. Kent Moore, University of Toronto for their assistance and providing data. Dr. Tada provided GANAL data and Dr. A. Segami of JMA supported to use JSM. We would like to express special thanks to them as well as staff members of the Numerical Prediction Division of JMA. The simulations and calculations of this work were performed using the Hitac S3800 super computer and the M880 computer at the Computer Center of the University of Tokyo and using IBM Power STATION RS6000/590 of ORI. The Grid Analysis and Display System (GrADS) developed at COLA, University of Maryland was used for displaying data and drawing figures.

A part of this project was supported by 'A Grant-in-Aid for Scientific Research, International Scientific Research Program' of the Ministry of Education, Science, Sports and Culture (Monbusyo), Japan.

References

Asai, T. and Y. Miura, 1981. An analytical study of meso-scale vortex-like disturbances observed around Wakasa Bay area. J. Meteor. Soc. Japan, **59**, 832-843.

Bratseth, A.M., 1985. A note on CISK in polar air masses. Tellus, **37A**, 403-406.

Businger, S., 1985. The synoptic climatology of polar low outbreaks. Tellus, **37A**, 419-432.

Businger, S., 1987. The synoptic climatology of polar low outbreaks over the Gulf of Alaska and the Bering Sea. Tellus, **39A**, 307-325.

Businger, S. and G. Walter, 1988. Comma cloud development and associated rapid cyclogenesis over the Gulf of Alaska : A case study using aircraft and operational data. Mon. Wea. Rev., **116**, 1103-1123.

Craig, G. and Han-Ru Cho, 1988. Cumulus heating and CISK in the extratropical atmosphere. Part I : polar lows and comma clouds. J. Atmos. Sci., **45**, 2622-2640.

Duncan, C.N., 1977. A numerical investigation of polar lows. Quart. J. Roy. Meteor. Soc., **103**, 255-267.

Eady, E.T., 1949. Long waves and cyclone waves. Tellus, **1**, 33-52.

Forsythe, J.M. and T.H.V. Haar, 1996. A warm core in a polar low observed with a satellite microwave sounding unit. Tellus, **48A**, 193-208.

Harrold, T.W. and K.A. Browning, 1969. The polar low as a baroclinic disturbance. Quart. J. Roy. Meteor. Soc., **95**, 710-723.

Mailhot, J., D. Hanley, B. Bilodeau and O. Hertzman, 1996. A numerical case study of a polar low in the Labrador Sea. Tellus, **48A**, 383-402.

Mansfield, D.A., 1974. Polar lows: the development of baroclinic disturbances in cold air outbreaks. Quart. J. Roy. Meteor. Soc., **100**, 541-554.

Moore, G.W.K., M.C. Reader, J. York and S. Sathiyamoorthy, 1996. Polar lows in the Labrador Sea: A case study. Tellus, **48A**, 17-40.

Mellor, G.L. and T. Yamada, 1974. A hierarchy of turbulence closure models for planetary boundary layers. J. Atmos. Sci., **31**, 1791-1806.

Nakamura, N., 1988. Scale selection of baroclinic instability—Effects of stratification and nongeostrophy. J. Atmos. Sci., **45**, 3253-3267.

Ninomiya, K., 1989. Polar/comma-cloud lows over the Japan Sea and the Northwestern Pacific in winter. J. Meteor. Soc. Japan, **67**, 83-97.

Orlanski, I., 1986. Localized baroclinicity: a source for meso- α cyclones. J. Atmos. Sci., **43**, 2857-2885.

Økland, H., 1987. Heating by organized convection as a source of polar low intensification. Tellus, **39A**, 397-407.

Rasmussen, E., 1979. The polar low as an extratropical CISK-disturbance. Quart. J. Roy. Meteor. Soc., **105**, 531-549.

Rasmussen, E., 1985. A case study of a polar low development over the Barents Sea. Tellus, **37A**, 407-418.

Rasmussen, E.A. and M. Lystad, 1987. The Norwegian Polar Lows Project: A summary of the International Conference on Polar Lows, 20-23 May 1986. Oslo, Norway. Bull. Amer. Meteor. Soc., **68**, 801-816.

Reed, R.J. and W. Blier, 1986a. A case study of comma cloud development in the Eastern Pacific. Mon. Wea. Rev., **114**, 1681-1695.

Reed, R.J. and W. Blier, 1986b. A further study of comma cloud development in the Eastern Pacific. Mon. Wea. Rev., **114**, 1696-1708.

Reed, R.J. and C.N. Duncan, 1987. Baroclinic instability as a mechanism for the serial development of polar lows: a case study. Tellus, **39A**, 376-384.

Sardie, J.M. and T.T. Warner, 1983. On the mechanism for the development of polar lows. J. Atmos. Sci., **40**, 869-881.

Sardie, J.M. and T.T. Warner, 1985. A numerical study of the development mechanisms of polar lows. Tellus, **37A**, 460-477.

Segami, A., K. Kurihara, H. Nakamura, M. Ueno, I. Takano and Y. Tatsumi, 1989. Operational mesoscale weather prediction with Japan spectral model. J. Meteor. Soc. Japan, **67**, 907-924.

Takano, I., H. Nakamura and Y. Tatsumi, 1990. Non-linear normal mode initialization for a spectral limited-area model. J. Meteor. Soc. Japan, **68**, 265-280.

Takano, I. and A. Segami, 1993. Assimilation and initialization of a mesoscale model for improved spin-up of precipitation. J. Meteor. Soc. Japan, **71**, 377-391.

Tatsumi, Y., 1986. A spectral limited-area model with time-dependent lateral boundary conditions and its application to a multi-level primitive equation model. J. Meteor. Soc. Japan, **64**, 637-664.

Tsuboki, K. and G. Wakahama, 1992. Mesoscale cyclogenesis in winter monsoon air streams.: Quasi-geostrophic baroclinic instability as a mechanism of the cyclogenesis off the west coast of Hokkaido Island, Japan. J. Meteor. Soc. Japan, **70**, 77-93.